Defence Research Establishment Pacific
Centre de recherches pour la défense pacifique

DEFENCE RESEARCH ESTABLISHMENT PACIFIC

CFB Esquimalt, FMO Victoria, B.C. VOS 1BO

Technical Memorandum 88-25

A DAMAGE TOLERANCE ASSESSMENT OF BONDED REPAIRS TO CF-18 COMPOSITE COMPONENTS

PART I: ADHESIVE PROPERTIES

BY

A.J. Russell

December 1988

Approved by:

CHIEF

Research and Development Branch
Department of National Defence

Canada

ABSTRACT

The damage tolerance properties of three epoxy adhesives used in the manufacture and repair of the composite structure on the CF-18 aircraft are assessed. The resistance to both static fracture and fatigue crack growth are evaluated. Experimental variables include the mode of fracture (tension and shear), the fatigue load ratio, the test temperature and the method of bonding. Both the static and fatigue tests were found to rank the adhesives in the same order, viz. FM-300K superior to FM-300 superior to EA-9321. The fatigue testing revealed a tendency for delamination type failures to occur at low temperature, a situation likely to lead to non-conservative joint designs. The fatigue crack growth rate data are explained in terms of the failure mechanisms observed. The implication of these findings to the selection of repair adhesives for composite aircraft structure is discussed.

KEY WORDS: Repair, Bonded Joint, Adhesive, Epoxy, Fracture, Fatigue, Crack Growth, Damage Tolerance, Durability, Composite Materials, Graphite/Epoxy, Aircraft.

INTRODUCTION

Adhesive bonding is used extensively in both the manufacture and repair of composite structure on the CF-18 aircraft. Graphite/epoxy to titanium bonds are found in the stepped lap joints which attach the wing skins, horizontal stabilators and vertical stabilizers to the fuselage. Graphite/epoxy face sheets and closures are bonded to aluminum honeycomb in numerous components including the rudder, trailing edge flaps and horizontal stabilators. Adhesively bonded repairs can take various forms including a single lap joint patch for honeycomb sandwich structure, Figure 1(a), and a scarf joint configuration for damage to monolithic graphite/epoxy, Figure 1(b).

A well designed adhesive joint should be stronger than the adjoining structure. This is normally achieved by carrying out an elastic/plastic stress analysis which is based on the shear stress/shear strain response of the adhesive. This approach to designing adhesive joints was developed in part by McDonnell Douglas in the early seventies [1] and later refined by the US Air Force Primary Adhesively Bonded Structure Technology (PABST) program [2]. It is not current practice to carry out a damage tolerance assessment of bonded joints in the design phase although guidelines to minimize peel stresses are generally followed. This lack of a damage tolerance qualification of bonded joints arose in part from the PABST program in which it was concluded that a joint designed to have sufficient strength would not normally fail in fatigue and that the additional complexities of a da/dN analysis were not warranted [3].

There are several reasons why the question of damage tolerance of bonded joints should be re-assessed when looking at bonded repairs to the CF-18's graphite/epoxy:

- Current CF-18 repair adhesives are more brittle than the 120°C curing toughened epoxy film adhesives that were evaluated in the PABST program.

- In composite material joints the high shear stresses close to the bondline may result in failure of the composite adherends. Under these conditions,

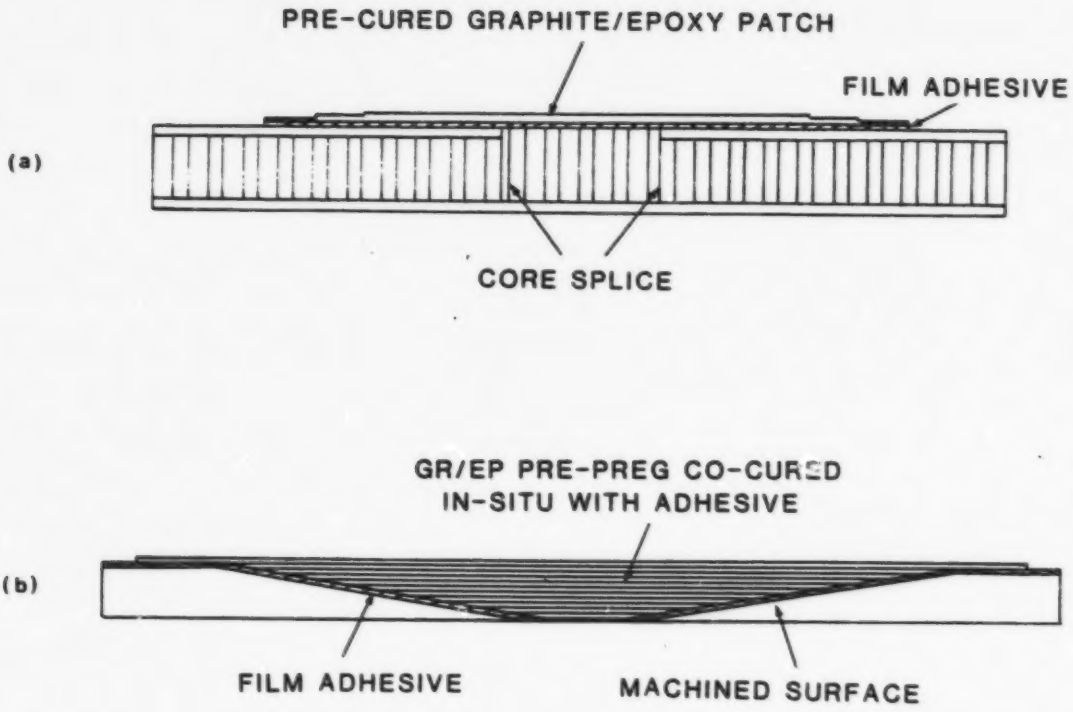

Figure 1. Examples of adhesively bonded repairs. (a) Surface patch bonded to honeycomb sandwich. (b) Scarf repair of monolithic laminate.

joints designed on the basis of the adhesive properties alone may be non-conservative.

- Previous fatigue crack propagation studies have not looked at worst case conditions in terms of both loading mode and environmental effects.

- Repairs are subject to additional constraints such as limitations on the size and weight of the patch, on changes in the local stiffness and on perturbation to the airflow. Consequently, the best possible repair may not have the same degree of strength redundancy as a typical production joint.

In this report, the growth of cracks between graphite/epoxy adherends bonded with the CF-18 adhesives will be investigated under both static and fatigue loading. The principle variables which will be examined are the test temperature, the fatigue load ratio, R, and the method of joint fabrication. The resulting data base will be used, in a subsequent report, to assess the damage tolerance of some typical composite repair schemes. In addition, future work will also make use of this data base for comparing other adhesive systems possessing secondary characteristics of special value in a repair situation.

EXPERIMENTAL

Materials and Fabrication

Table 1 describes the CF-18 adhesives used either in production or specified in the Structural Repair Manual (SRM). The two film adhesives, FM-300 and FM-300K differ only in their colour and the type of scrim cloth. Neither EA-956, which is an unfilled version of EA-9321, nor the foaming adhesive FM-404 have been included in this test program. The film adhesives were tested both bonded and co-cured whereas EA-9321 was bonded only, simulating current practice.

TABLE 1

CF-18 Adhesive Materials

Name and Supplier	Type of adhesive	Application	Bonding Procedure
FM-300 American Cyanamid	Epoxy film on tightly knitted scrim cloth.	Gr/Ep face sheets to closures and honeycomb core.	Secondary bonding 1 hour at 178°C, 32-50 psi, vent vacuum.
		Repair patch to graphite/ epoxy H/C sandwich with B-staged adhesive.	Secondary bonding 4 hours at 149°C, 20-29" Hg vacuum.
		Scarf joint repair to Gr/ Ep H/C sandwich.	Co-cured with pre-preg 2 hours at 178°C, 100 psi.
FM-300K American Cyanamid	Epoxy film on open knit scrim.	Gr/Ep to titanium step-lap joints.	Co-cured with pre-preg 2 hours at 178°C, 100 psi.
EA-9321 Hysol	2 part epoxy with thickener.	Repair patch to graphite/ epoxy skin.	Secondary bonding 1 hour at 88°C, 20-29" Hg vacuum.
EA-956 Hysol	2 part epoxy	Repair of delaminations.	1 hour at 88°C, 20-29" Hg vacuum.
FM-404 American Cyanamid	Foaming adhesive film.	Core stabilisation during manufacture and at repair splices.	1 hour at 178°C or 4 hours at 149°C.

Test laminates, of either 24 or 36 unidirectional plies, were made from Hercules AS4/3501-6 graphite/epoxy and cured according to CF-18 specifications. For co-cured laminates both the top and bottom surfaces were bled to ensure that the adhesive lay on the mid-plane. Bonded laminates were fabricated from two 12 or 18 ply laminates. For the initial tests, the surface of the laminates to be bonded were lightly wet sanded with 600 grit abrasive paper until drops of water would no longer bead up on the surface. Later tests examined the effect of more heavily sanding the surface as detailed below.

Strips of 25 μm thick teflon coated glass fabric were incorporated into the laminates to act as crack starters. For EA-9321 the inserts were located at the centre of the bondline but for the film adhesives this was not possible and hence they were positioned adjacent to one side of the adhesive film. Specimens, 150 mm long by 20 mm wide, were machined from the laminates and stored in a desiccator until immediately prior to use. Tests were carried out in laboratory air at -50, 20 and 100°C.

Fracture Testing

Mode I and Mode II adhesive fracture tests were made with Double Cantilever Beam (DCB) and End Notched Flexure (ENF) specimens respectively. These specimens, shown in Figure 2, are essentially the same as those used for previous delamination studies [4] and consequently similar testing procedures were employed. The ram displacement rate was 10 mm/min for the DCB tests and 2 mm/min for the ENF tests.

Fatigue Testing

Cyclic debonding tests under pure shear loading were carried out on End Notched Cantilever Beam (ENCB) specimens as shown in Figure 3. This loading arrangement is similar to that used previously to study interlaminar fatigue crack growth [5]. The span L, was 110 mm, with the debond growing from an initial length of 35 mm to a final value of between 100 and 105 mm.

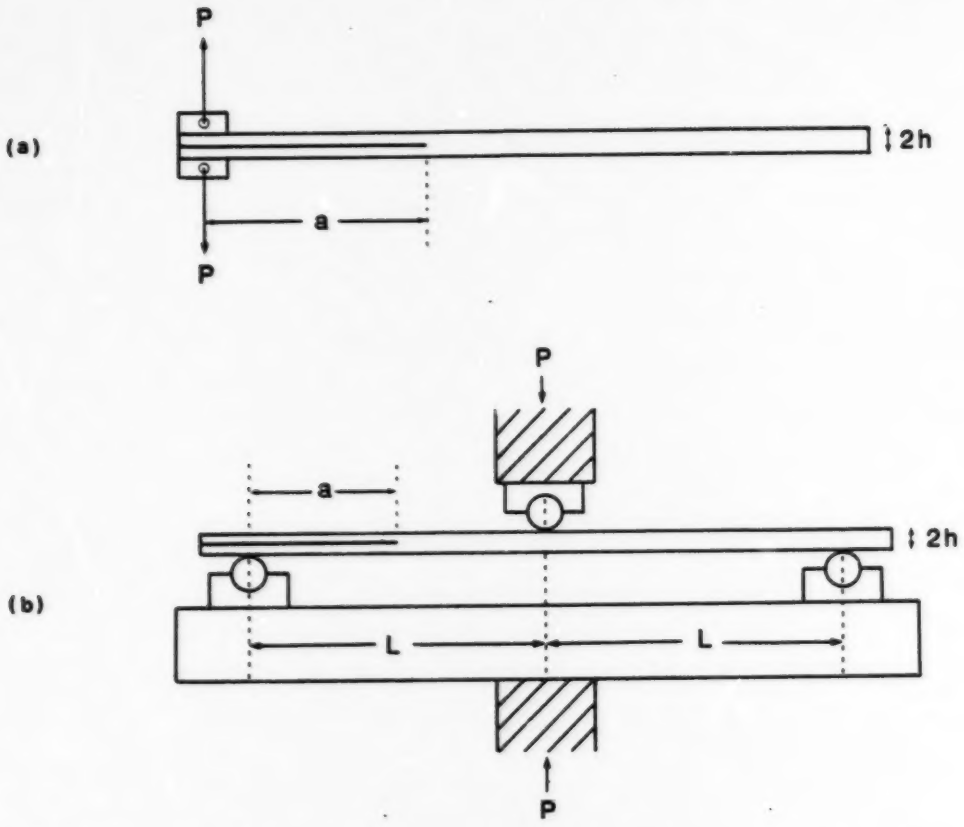

Figure 2. Fracture specimens. (a) Double Cantilever Beam test for Mode I. (b) End Notched Flexure Test for Mode II.

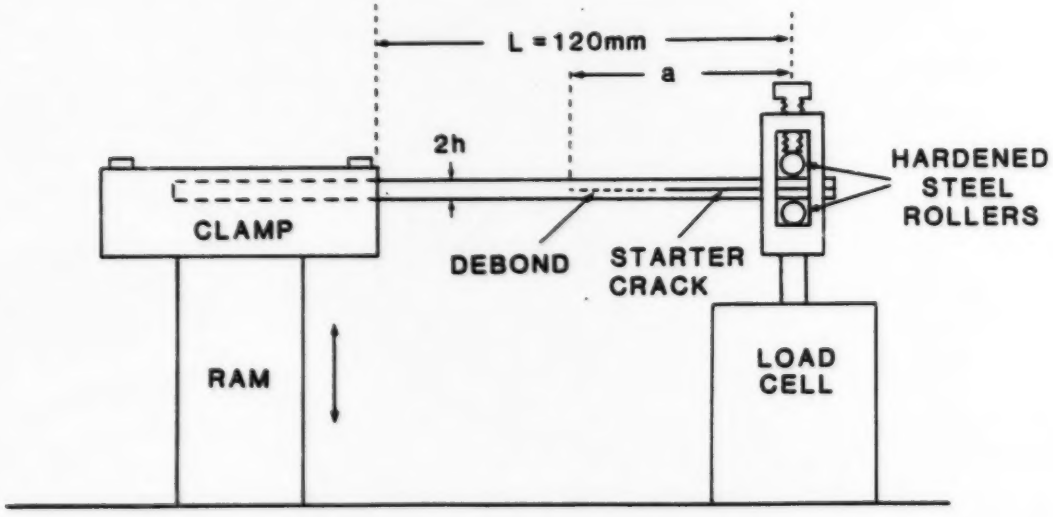

Figure 3. End Notched Cantilever Beam test for Mode II fatigue.

All tests were run in stroke control on a fully automated MTS load frame with an 800 N load cell. Blocks of constant amplitude sine-wave cycles were separated by slow ramp cycles of the same amplitude during which the specimen compliance was measured. The maximum and minimum values of the load, P, and load-point displacement, δ, were measured during the last ten cycles of each block and the average values stored.

Most tests were run at either 2 Hz and an R-ratio of 0 (forward shear) or at 1 Hz and an R-ratio of -1 (reverse shear). Following completion of a test the specimen was separated into two halves and the initial and final crack lengths measured from markings on the fracture surface.

DATA REDUCTION

Fracture Tests

For the mode I fracture tests the following closed form expression was used to calculate the mode I fracture energy, G_{Ic} [4],

$$G_{Ic} = \frac{3CP_c^2}{2ab} \tag{1}$$

where C is the loading compliance of the specimen
P_c is the load at fracture
a is the crack length
and b is the specimen width.

The equation for calculating the mode II fracture energy, G_{IIc} for the ENF specimen was modified to take into account the presence of the adhesive [6].

$$G_{IIc} = \frac{9P^2\alpha a^2 C}{2b(2L^3 + 3\alpha a^3)} \tag{2}$$

where $\alpha = 1+4t/(h-t)$
t is the adhesive thickness
and h is the specimen half thickness.

Fatigue Tests

The crack length corresponding to each compliance measurement was calculated from Equation 3,

$$C = \frac{C_f(a^3 - a_i^3) + C_i(a_f^3 - a^3)}{a_f^3 - a_i^3} \qquad (3)$$

where a is the crack length
C is the compliance
and $_i$ and $_f$ refer to the initial and final values respectively,

and the strain-energy release rate, G_{II}, calculated from Equation 4,

$$G_{II} = \frac{3(C_i - C_f)a^2P^2}{2b(a_i^3 - a_f^3)} \qquad (4)$$

where, P is the load.

Next, the crack growth rate, da/dN, corresponding to each crack length was determined by least squares fitting a third order polynomial to the crack length, a, versus number of cycles, N, data. For each specimen, G_{II} increased initially due to the increasing crack length, then reached a maximum at $a/L \simeq 0.6$ after which it declined due to the decreasing load. Thus each specimen gave two values of da/dN over a limited range of G values. Several specimens tested at different constant amplitudes were required to produce a log da/dN versus log ΔG_{II} plot covering 3 or 4 decades of crack growth rate. For all plots $\Delta G_{II} = G_{max} - G_{min}$ and for both R=0 and R=-1, G_{max} corresponds to P_{max} and G_{min} corresponds to zero load following the convention adopted by reference 5.

RESULTS

Fracture Tests

In Figures 4-6 an example is shown of the mode I load-displacement (P-δ) curves for each adhesive at each test temperature. All materials displayed linear behaviour up to the initiation of crack growth

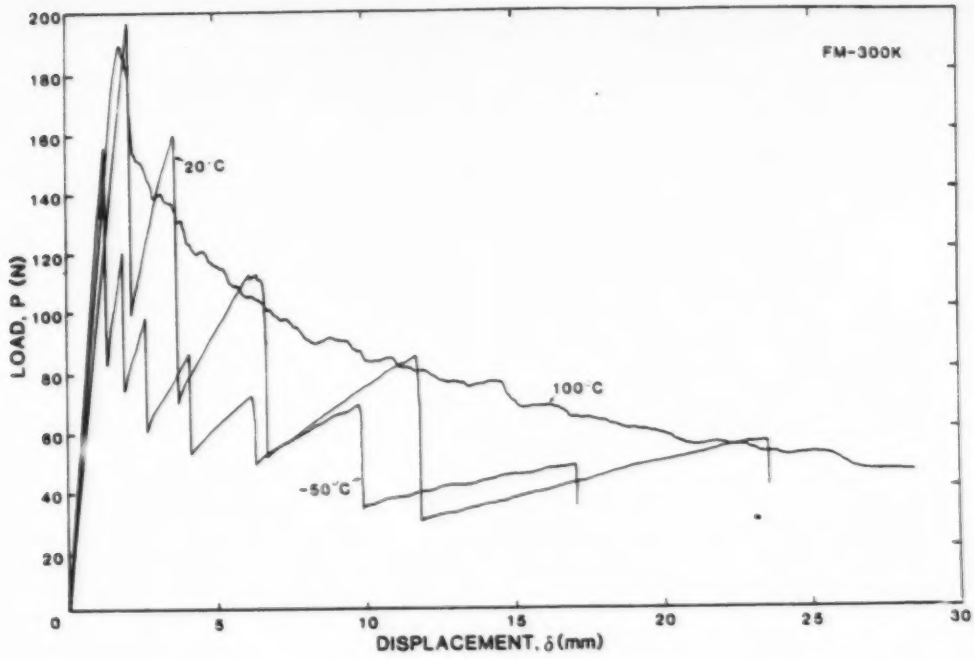

Figure 4. Examples of P-δ curves for Mode I fracture of FM-300K at different test temperatures.

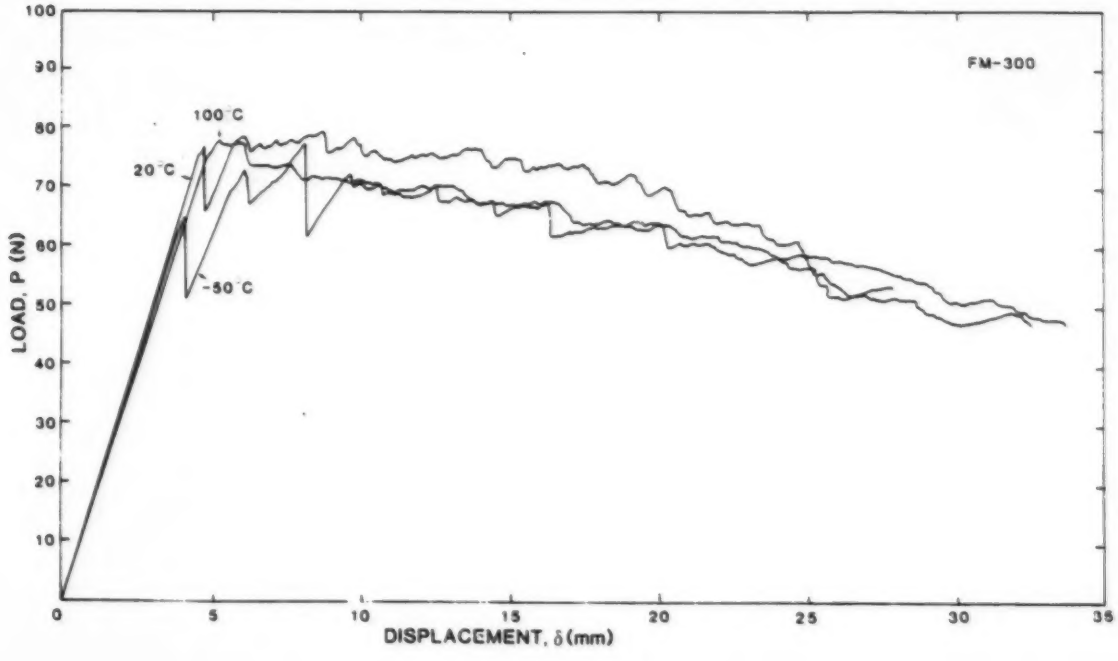

Figure 5. Examples of P-δ curves for Mode I fracture of FM-300 at different test temperatures.

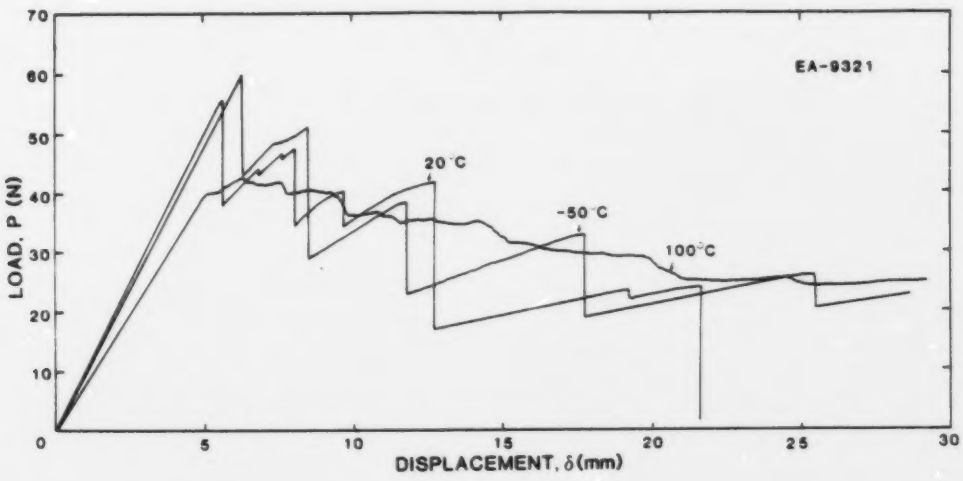

Figure 6. Examples of P-δ curves for Mode I fracture of EA-9321 at different test temperatures.

followed by varying degrees of slip/stick crack propagation at low temperatures and stable crack growth at higher temperatures. The general shape of the P-δ plots for FM-300K and EA-9321 indicates that the fracture energy remained relatively constant as the debond extended. However, in the FM-300 specimens the fracture energy was found to increase as evidenced by the plateau like nature of the P-δ curves. This increase was due to the stretching of the scrim cloth between the fracture surfaces behind the crack tip as it failed to separate cleanly from the epoxy.

In Figure 7 the mode I fracture energies are plotted as a function of temperature for all three adhesives. The values given for FM-300 correspond to the initial (or minimum) fracture energy only, whereas the results for the other two adhesives are averaged over the total length of debond extension. Where slip/stick (or initiation/arrest) behaviour was observed, the values shown correspond to crack initiation. All failures were cohesive within the adhesive itself and no difference was observed between bonded and co-cured specimens.

Figures 8-11 show the corresponding results for mode II fracture. All of the P-δ curves showed a significant amount of non-linear behaviour prior to fracture with the exception of the EA-9321 at -50°C. At 100°C none of the curves was sufficiently linear to allow the use of linear elastic fracture mechanics to calculate G_{IIc}. Fracture energies are given in Figure 11 where appropriate, otherwise an estimate of the work of fracture [7] is given instead. No rigorous non-linear treatment of the P-δ curves was undertaken for reasons that will be discussed below. All fracture surfaces indicated cohesive failure modes and once again there was no difference between bonded and co-cured specimens.

Fatigue Tests

Most of the fatigue tests were carried out on FM-300K and EA-9321 adhesives with only limited testing of FM-300. This was because of the history dependent behaviour caused by the partial debonding of the FM-300 scrim cloth as described below.

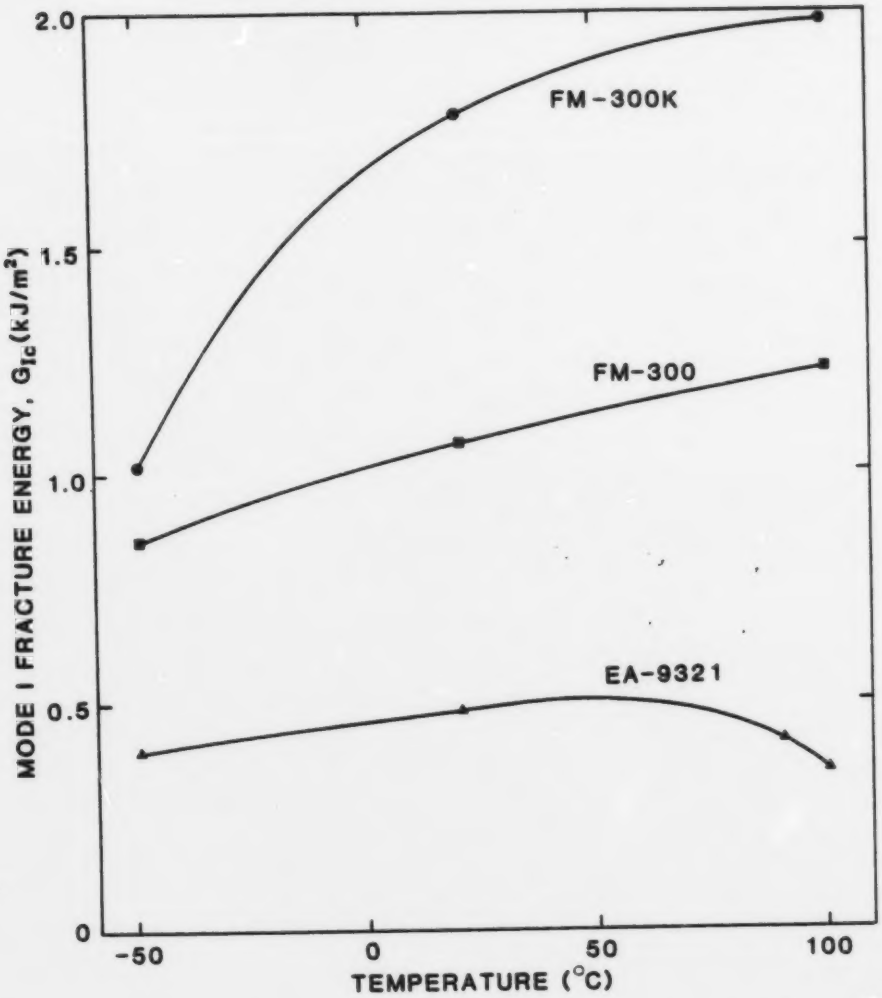

Figure 7. Effect of temperature on the Mode I adhesive fracture energy.

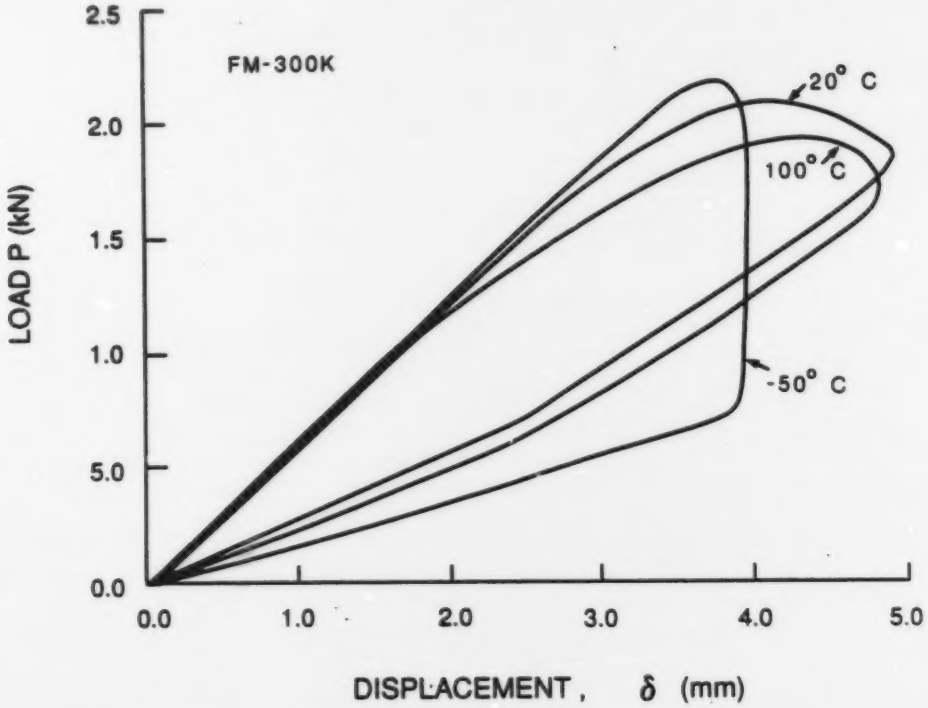

Figure 8. Examples of P-δ curves for Mode II fracture of FM-300K at different test temperatures.

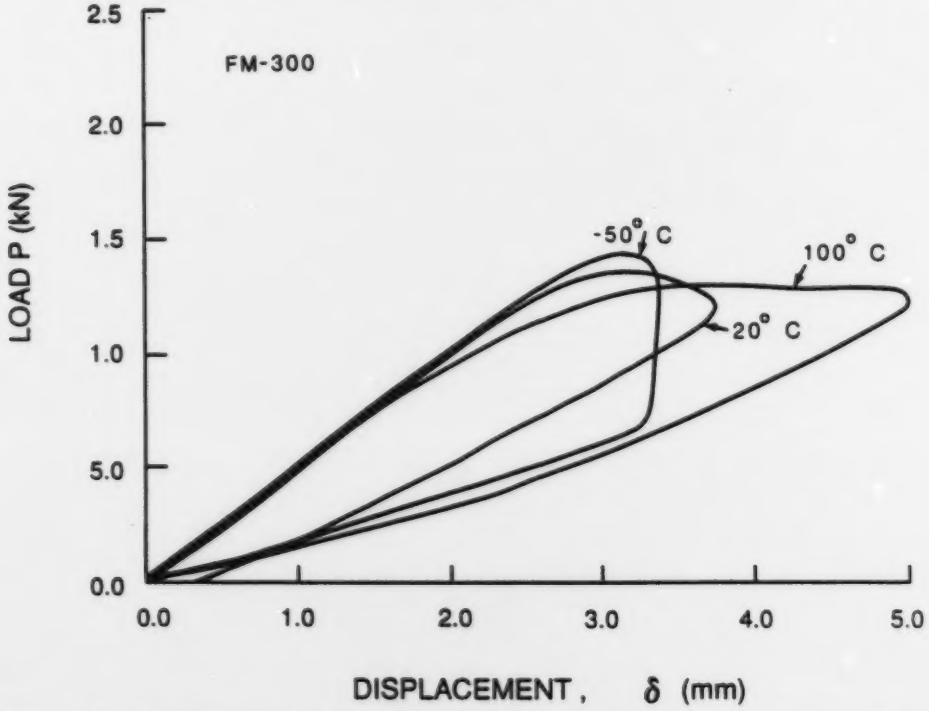

Figure 9. Examples of P-δ curves for Mode II fracture of FM-300 at different test temperatures.

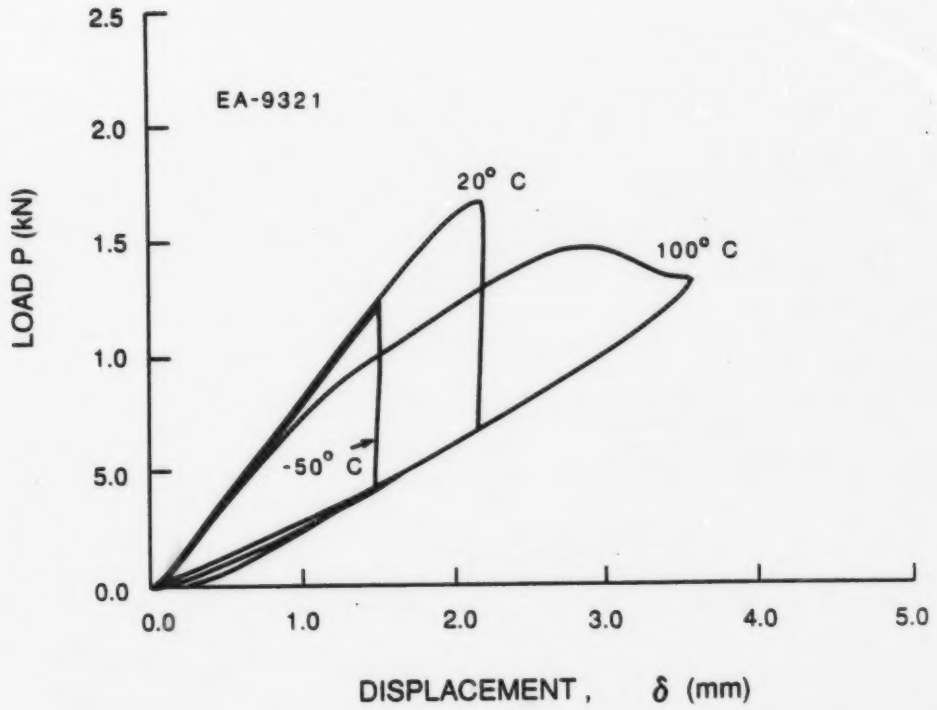

Figure 10. Examples of P-δ curves for Mode II fracture of EA-9321 at different test temperatures.

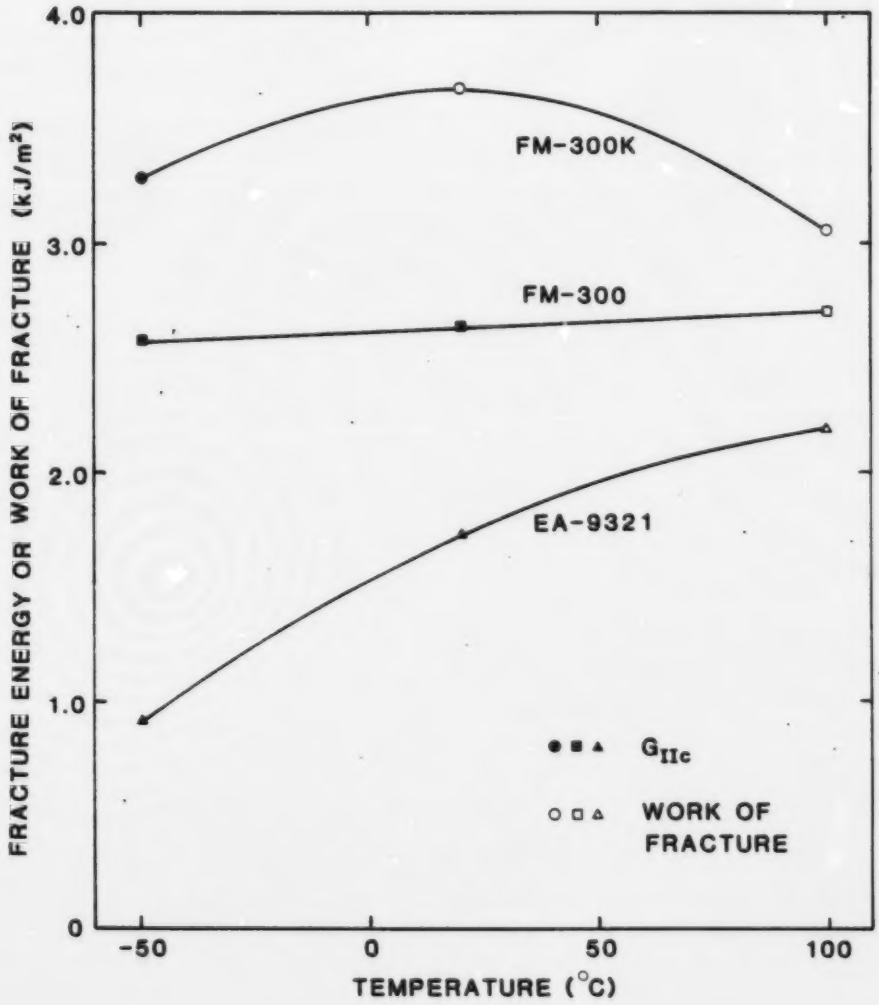

Figure 11. Effect of temperature on the Mode II adhesive fracture energy or work of fracture.

Effect of Frequency

The sensitivity of the cyclic debonding behaviour to test frequency was investigated over the range 0.1 to 4 Hz. These tests were run on co-cured FM-300K specimens at 100°C and R = -1 as it was felt that these would best reveal evidence of any strain rate sensitivity. The results plotted in Figure 12 indicate that there was no significant frequency effect.

Effect of Temperature

Figures 13 and 14 show the effect of temperature on FM-300K and EA-9321 for R=-1. Raising the temperature increased the fatigue crack growth rates in both the co-cured FM-300K specimens and the bonded EA-9321 specimens. However, the situation was more complex in the bonded FM-300K samples where the failure path moved from the adhesive at elevated temperatures to the composite matrix at low temperatures [6]. At 20°C both failure modes were observed, with a transition from one mode to the other occurring between 0.2 and 0.4 kJ/m^2. Comparing Figures 13 (a) and (b) reveals that failure through the epoxy matrix on the surface of the adherends has led to a substantial reduction in the ΔG values required for fatigue crack growth at -50°C. As a result of this finding additional tests were undertaken to ascertain the effect of removing the surface matrix layer on the composite adherends prior to bonding. An examination of the EA-9321 specimens tested at -50°C revealed that at low ΔG values they too had failed via surface matrix layer cracking.

Effect of Removing Surface Matrix Layer

Two different sanding procedures were investigated in determining the effect of removing the surface matrix layer in the FM-300K specimens. The first involved wet sanding with successively finer and finer grits finishing with a 600 grit paper until all damage from the coarser grits had been removed. The second method was similar to that used for preparing scarf joint repairs at the Naval Air Rework Facility (NARF). A belt sander

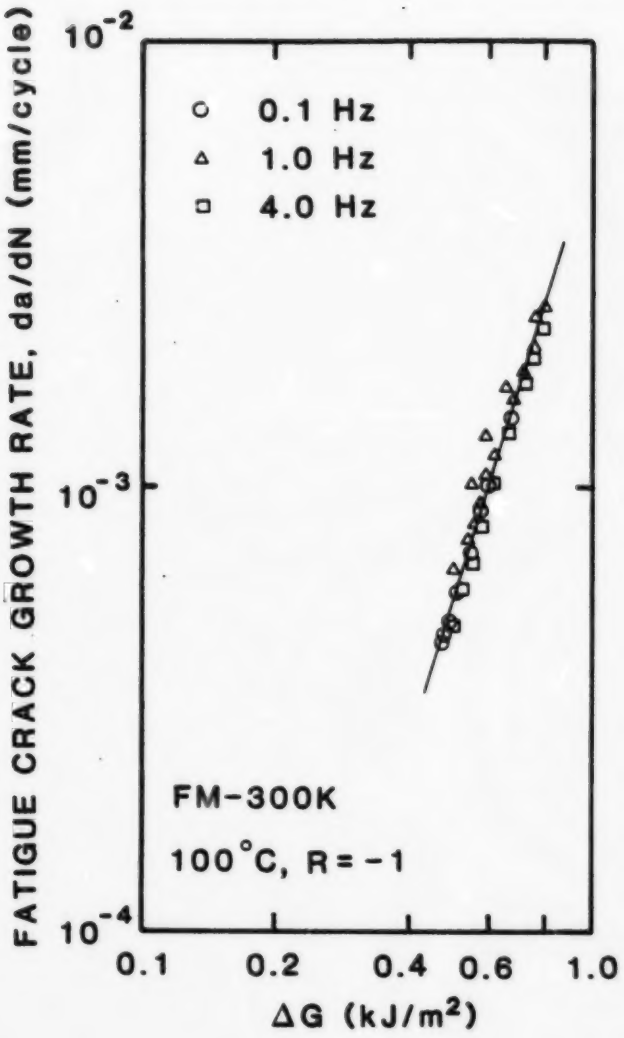

Figure 12. Effect of frequency on the fatigue crack growth rate of FM-300K at 100°C.

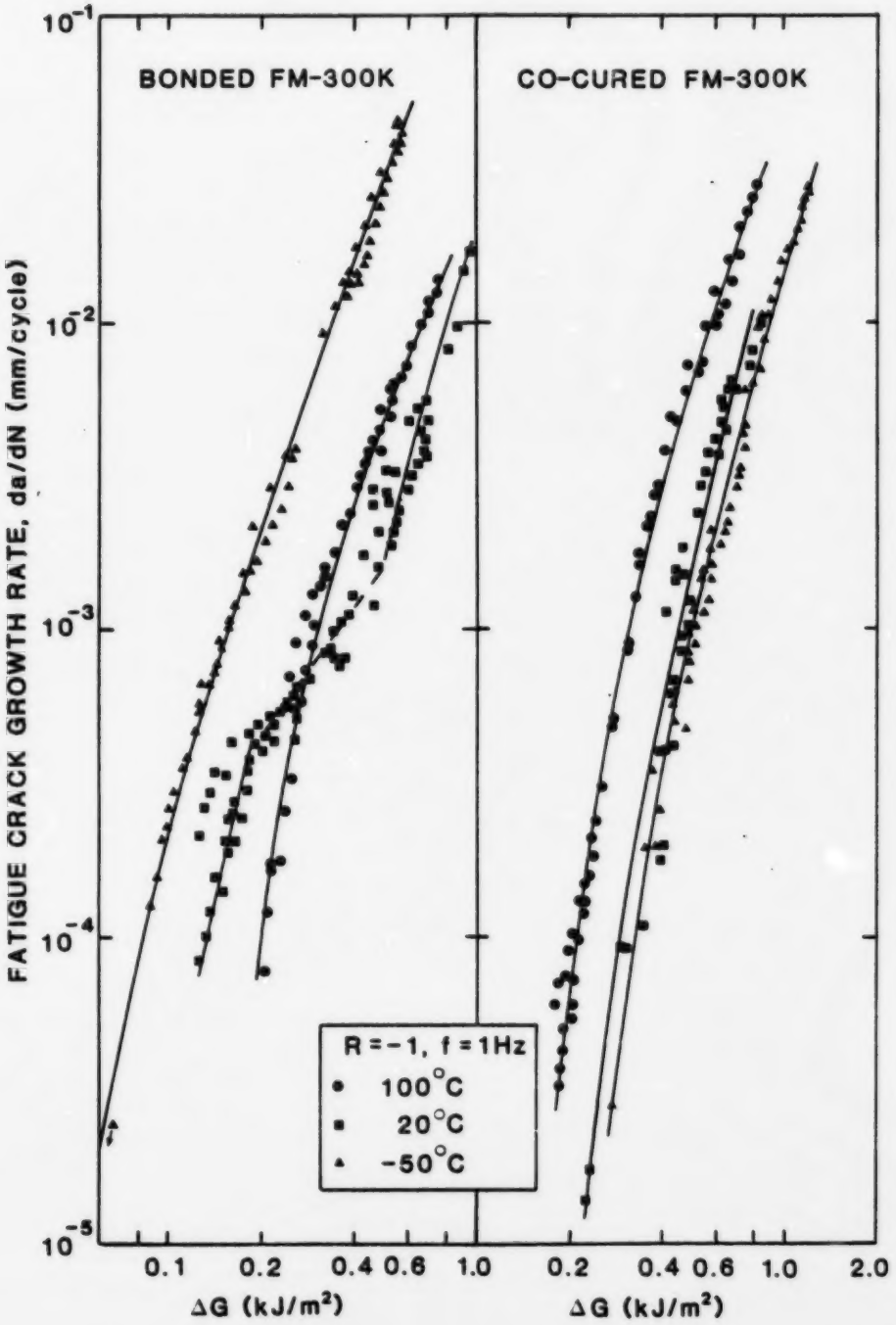

Figure 13. Effect of temperature on the fatigue crack growth rate of FM-300K.

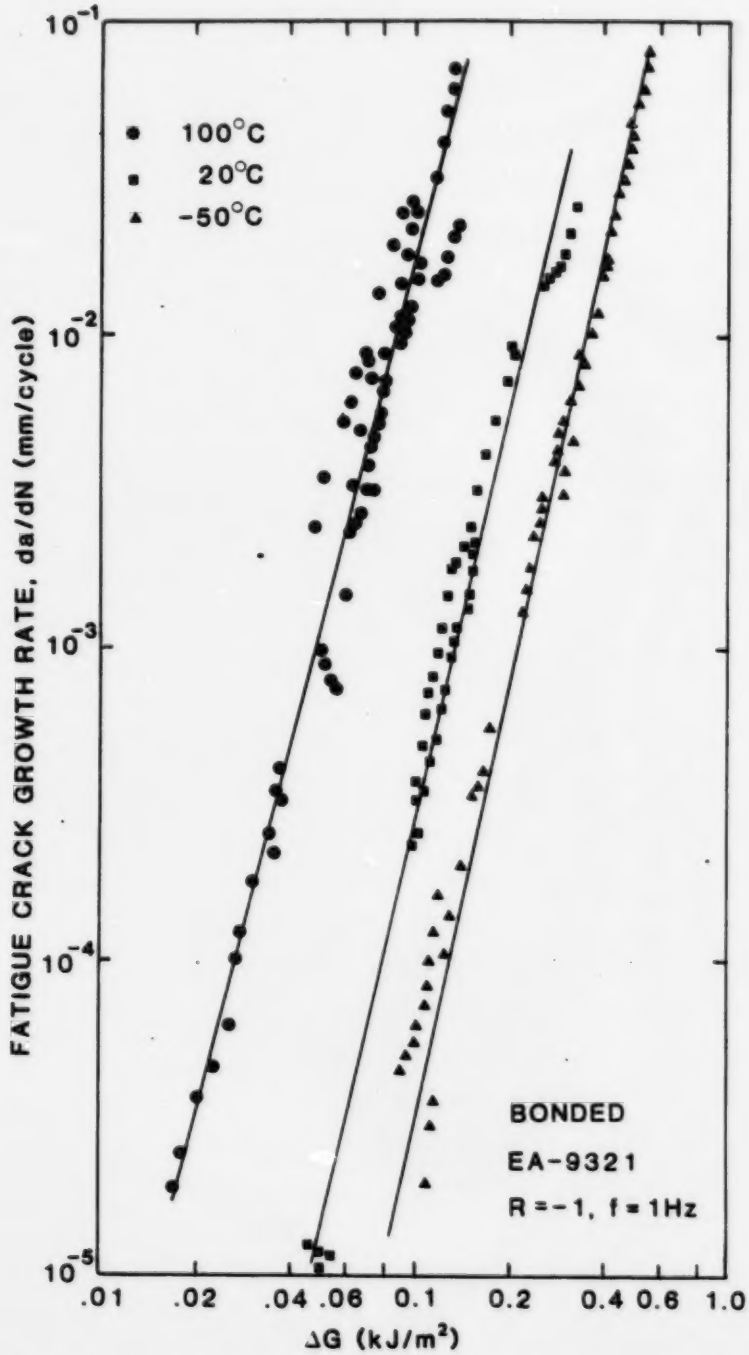

Figure 14. Effect of temperature on the fatigue crack growth rate of EA-9321.

with an 80 grit paper was used to obtain the desired amount of surface removal finishing with a wipe from a dry cloth to remove any excess dust.

Figure 15 indicates that both methods resulted in a significant shift in the da/dN versus ΔG curves to higher ΔG values although neither procedure was able to achieve the superior fatigue resistance of the co-cured joints. The wet sanding was slightly superior at higher ΔG values as reflected in the fracture surfaces which showed fewer broken fibres on the adhesive face, indicative of less delamination.

Effect of R-ratio

The enhanced fatigue crack growth rates due to shear reversal (R=-1) are compared with the da/dN values for positive shear only (R=0) in Figure 16. The curves for EA-9321 and co-cured FM-300K at 100°C display a greater effect of R-ratio than either of the -50°C tests shown.

Comparison of FM-300 with FM-300K

Figures 17 (a) and (b) show the da/dN versus ΔG curves for several FM-300 specimens at 20°C and 100°C. Unlike the data for FM-300K and EA-9321 the data points for the individual specimens do not fall back on top of themselves as ΔG increases to a maximum and then diminishes. Instead, as the debond grows, the resistance to fatigue crack growth increases resulting in the type of da/dN versus ΔG curves shown. Because of this history dependent behaviour only a limited number of tests were run on the FM-300 specimens. When compared with the corresponding results for FM-300K (dashed curves in Figure 17) it is apparent that fatigue crack growth initiates in the FM-300 specimens at significantly lower ΔG values.

DISCUSSION

The results of both the mode I and mode II static tests as well as the mode II fatigue tests rank the adhesives in the same order, i.e. FM-300K is better than FM-300 which is better than EA-9321. The superior

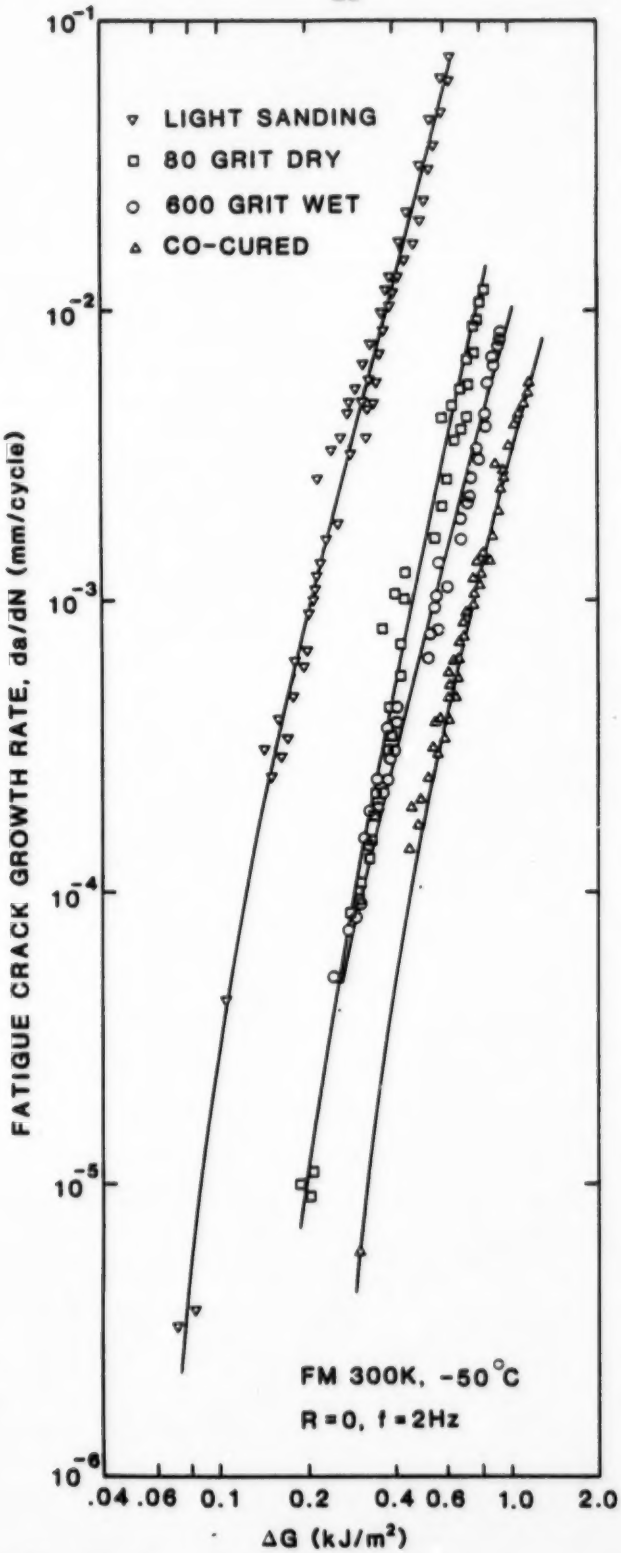

Figure 15. Effect of bonding procedure on the fatigue crack growth rate of FM-300K at -50°C.

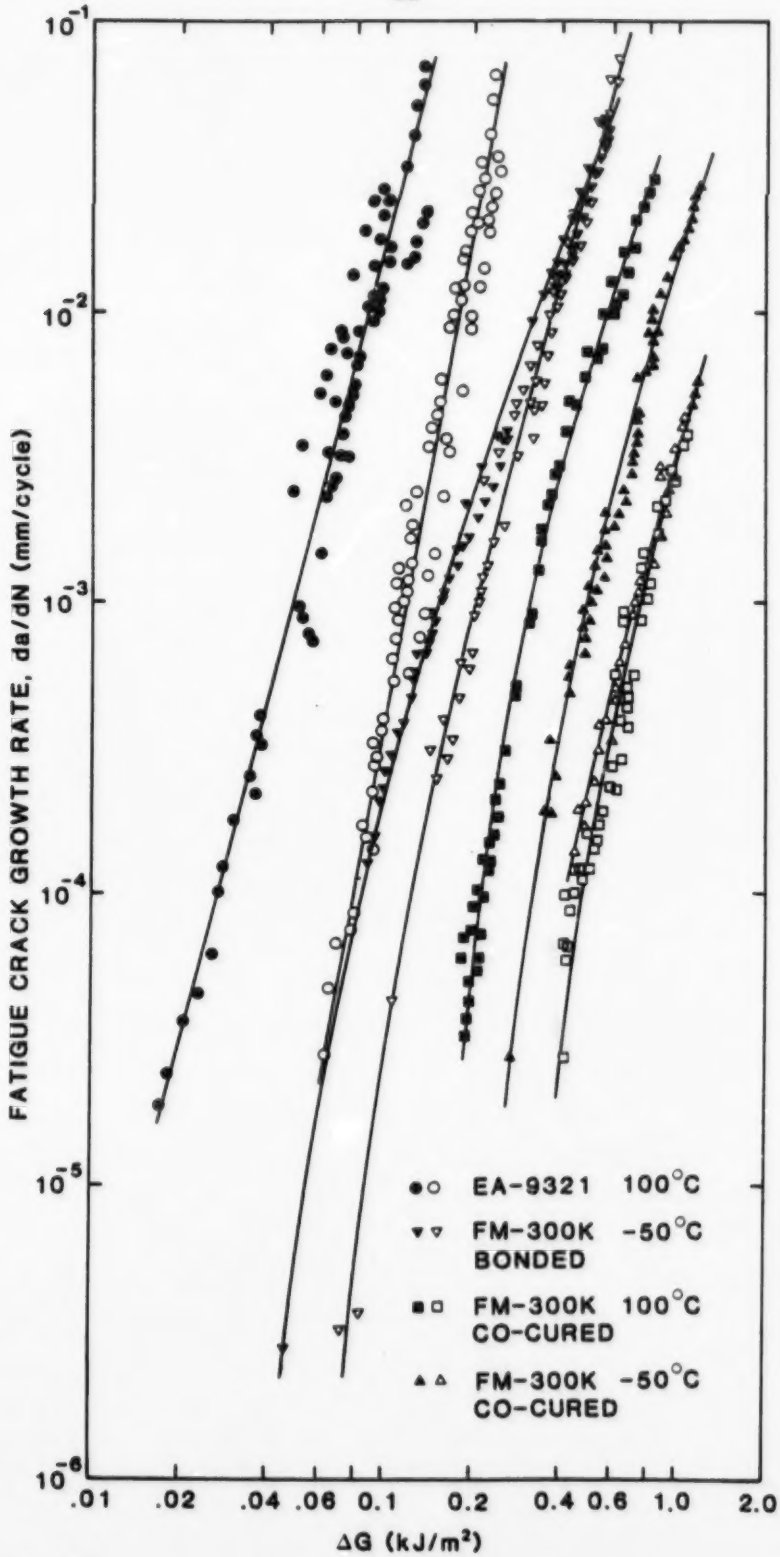

Figure 16. Effect of R-ratio on the fatigue crack growth rate of FM-300K and EA-9321. Open symbols: R=0. Solid symbols: R=-1.

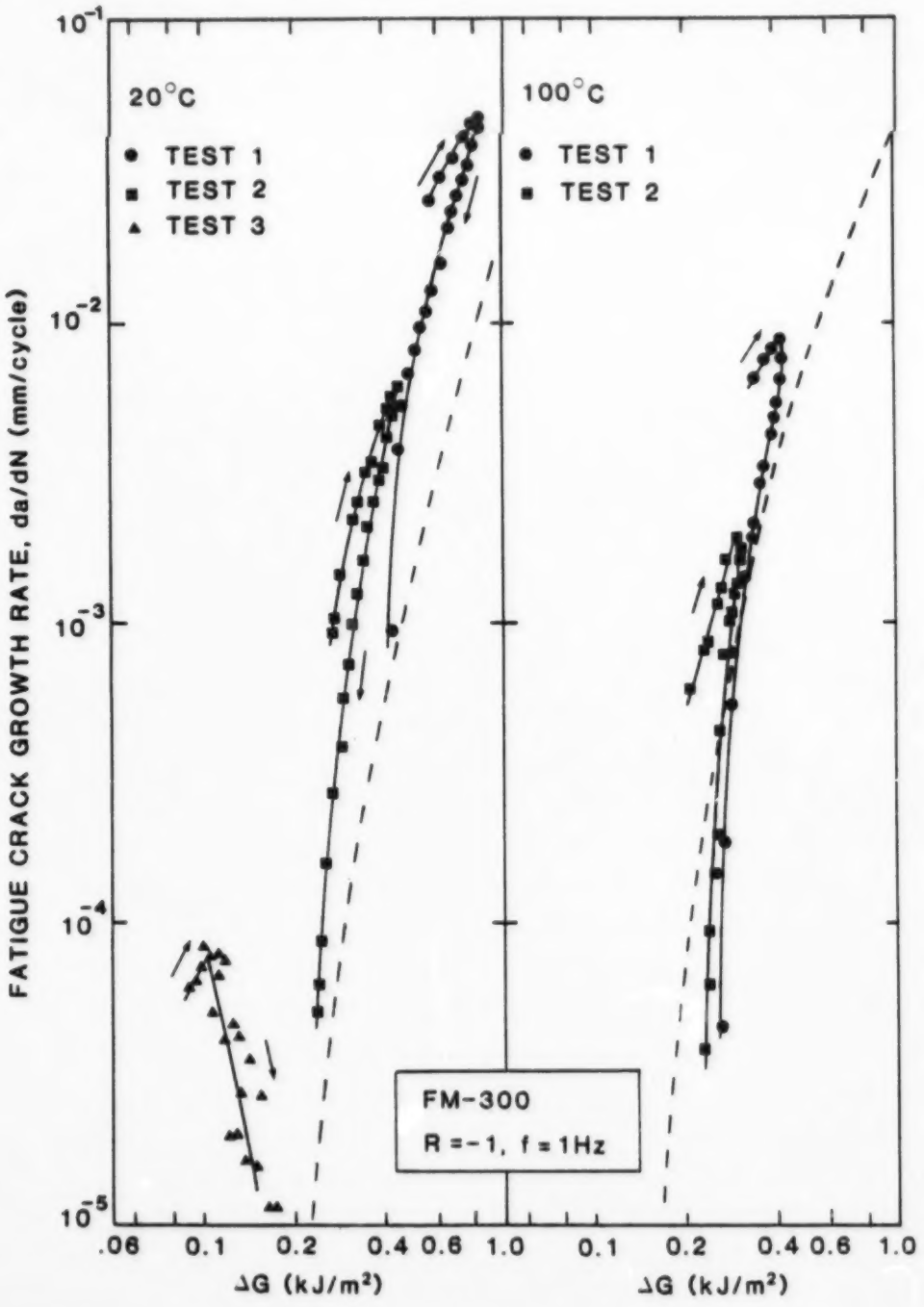

Figure 17. Comparison of fatigue data for co-cured FM-300 at 20°C and 100°C with FM-300K curves (dashed lines). Arrows indicate direction of test progression.

performance of the two film adhesives was expected and is a direct consequence of their greater rubber content. The reduced performance of FM-300 compared with FM-300K was not anticipated although a similar deteriorating effect of a closed knit scrim cloth has been observed for FM-1000 type adhesives [8]. The thicker scrim in FM-300 was dictated by the need to prevent electrical contact between graphite fibres and aluminum honeycomb, a situation likely to lead to galvanic corrosion of the core. Based on the present results, it would appear that the use of FM-300K would be preferable to FM-300 except when bonding to aluminum core. This would include the scarf repair in Figure 1(b) as well as the patch-to-skin part of the repair in Figure 1(a). However, in some situations the greater flow of the FM-300 (greater initial thickness but similar cured thickness) is beneficial as it is more forgiving of two poorly fitting surfaces. The use of two layers of FM-300K film in such circumstances might be worthy of future investigation.

The P-δ curves indicated that all three adhesives behaved in a more brittle manner as the temperature was lowered to -50°C although this did not always correspond to the minimum fracture energy or work of fracture. The reason for this is that while all the adhesives showed greater ductility at elevated temperature their ability to sustain high shear stresses is also reduced and in energy terms this may override the increased strain to failure. In contrast, the fatigue crack growth rate was greatest at elevated temperatures. The only exception was in the case of the bonded FM-300K specimens where cracking occurred in the surface matrix layer of the graphite/epoxy adherends at low temperature. Not only was this the worst case condition for fatigue growth, the change in failure mode means that design methodologies based on adhesive properties alone will be non-conservative. Failures of adhesively bonded composite joints by delamination have generally been attributed to peel stresses [9]. However, the present results show that shear stresses alone can cause "interlaminar" failure.

For all three adhesives, fatigue crack growth occurred at ΔG values substantially below G_{IIc}. A fatigue threshold, ΔG_{th} has been defined as the strain energy release rate below which no fatigue growth occurs [10].

No special effort was made to measure ΔG_{th} in this investigation. However, approximate values can be estimated by extrapolating the da/dN versus ΔG curves down to 10^{-6} mm/cycle. Some of these values for the R=-1 tests are shown as a percentage of G_{IIc} in Figure 18 and indicate that fatigue cracking can occur at ΔG values as low as 1% of the fracture energy.

Ideally, a damage tolerant repair (in addition to being stronger than the surrounding structure) should be designed in such a manner that no fatigue growth would occur even with a debond type flaw present. Under these conditions the fracture energy of the adhesive would not be a factor in the design. For this reason, no non-linear analysis of the adhesive fracture behaviour was pursued in this investigation. The consequences of a "no growth" design methodology on some typical composite repair schemes will be analysed in part 2 of this report.

CONCLUSIONS

(1) The film adhesives FM-300 and FM-300K are substantially more damage tolerant than the paste adhesive EA-9321 because of the greater ductility imparted by their higher rubber content. This is especially true at elevated temperature.

(2) FM-300 is less damage tolerant than FM-300K due to the close knit scrim cloth debonding from the adhesive.

(3) Joints formed by secondary bonding are less durable than co-cured joints due to the presence in the former of a relatively less fatigue resistant matrix layer adjacent to the bond line.

(4) Removal of the surface matrix layer of the composite prior to bonding can raise the threshold for fatigue growth at low temperatures by as much as a factor of two.

(5) Shear reversal (R=-1) increases the sensitivity to fatigue crack growth compared to forward shear (R=0) alone. This is especially true at elevated temperature.

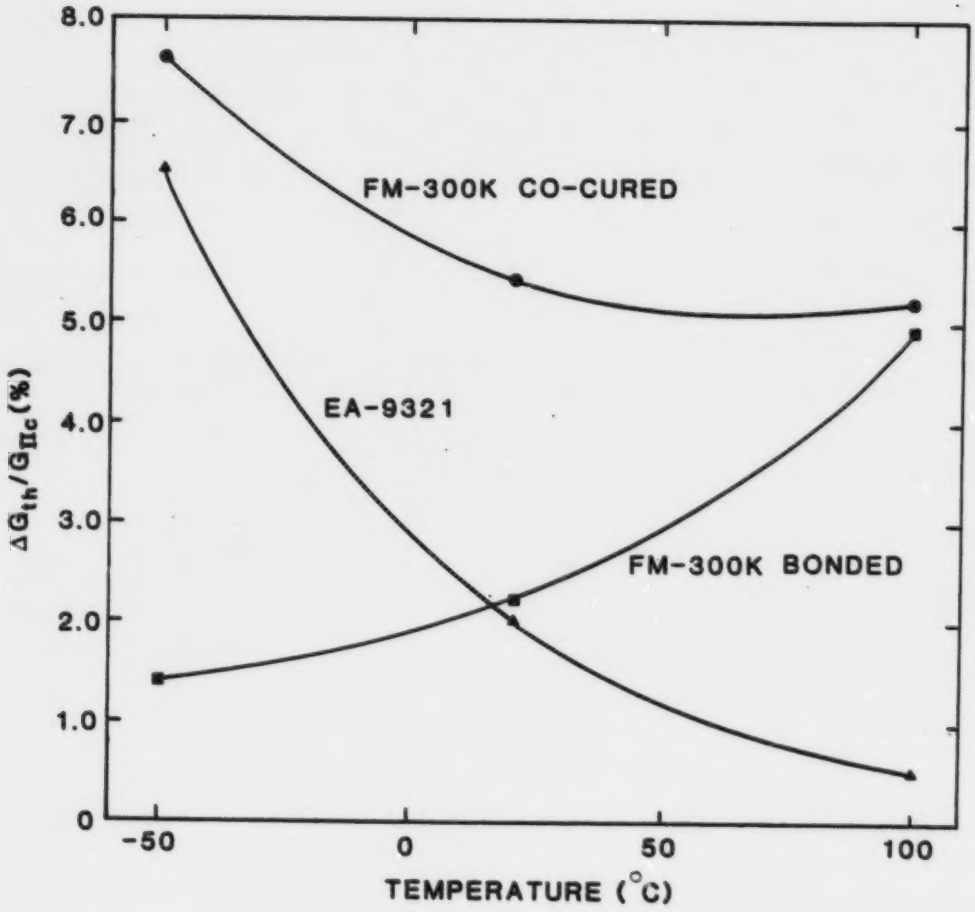

Figure 18. Fatigue thresholds normalized with respect to fracture energy as a function of temperature for FM-300K and EA-9321.

(6) Thresholds for fatigue crack growth are typically between 1 and 10 percent of G_{IIc} for R=-1, indicating a strong sensitivity to fatigue loading.

ACKNOWLEDGEMENTS

The support and encouragement of Dr. K. N. Street as well as the skilled technical assistance of E. Jensen are both gratefully acknowledged.

REFERENCES

1. L.J. Hart-Smith, "Analysis and Design of Advanced Composite Bonded Joints", Douglas Aircraft Company, NASA CR-2218, Jan. 1973.

2. L.J. Hart-Smith, "Adhesive-Bonding of Aircraft Primary Structure", Douglas Aircraft Company, MDC Paper 6979, 1980.

3. L.J. Hart-Smith, "Design and Analysis of Bonded Repairs for Metal Aircraft Structures", Douglas Aircraft Company, Douglas Paper 7089, 1981.

4. A.J. Russell and K.N. Street, "Moisture and Temperature Effects on the Mixed-Mode Delamination Fracture of Unidirectional Graphite/Epoxy" STP 876 on Delamination and Debonding, ASTM, Philadelphia, 1985, pp 349-370.

5. A.J. Russell and K.N. Street, "The Effect of Matrix Toughness on Delamination", STP 937 on Toughened Composites, ASTM, Philadelphia, 1987, pp 275-294.

6. A.J. Russell, "Fatigue Crack Growth in Adhesively Bonded Graphite/Epoxy Joints",Proc. ASME Symposium on Advances in Adhesively Bonded Joints, Chicago, 1988.

7. A.J. Russell, "On the Measurement of Mode II Interlaminar Fracture Energies", DREP Materials Report 82-0, Dec. 1982.

8. D.M. Brewis, J. Comyn, B.C. Cope and A.C. Moloney, "Effect of Carriers on the Performance of Aluminum Alloy Joints Bonded with an Epoxide-Polyamide Adhesive", Polymer, 21, 1980, pp 344-351.

9. L.J. Hart-Smith, "Adhesively Bonded Joints for Fibrous Composite Structures", Douglas Aircraft Company, Douglas Paper 7740, 1986.

10. W.S. Johnson and S. Mall, "A Fracture Mechanics Approach for Designing Adhesively Bonded Joints", STP 876 on Delamination and Debonding, ASTM, Philadelphia, 1985, pp 189-200.

DISTRIBUTION

REPORT NUMBER: DREP Technical Memorandum 88-25

TITLE: A Damage Tolerance Assessment of Bonded Repairs to CF-18 Composite Components. Part I: Adhesive Properties

AUTHOR: A. J. Russell

DATED: December 1988

SECURITY GRADING: UNCLASSIFIED

2 - DSIS

1 - CRAD
1 - C/DREA
1 - C/DREV
1 - C/DRES
1 - DRDA
1 - DRDL
1 - DRDM
1 - CDLS (W)
1 - CDLS (L)
1 - DRA (P)

1 - DAS Eng 6
1 - DAS Eng 6-3
1 - DAS Eng 3
1 - DFTEM 2
1 - PMO NSA (SEM)
1 - QETE
1 - AETE
1 - AMDU (MPB)
1 - NRC/NAE
1 - Canadair

BRITAIN

1 - DRIC

UNITED STATES

1 - DTIC

UNCLASSIFIED

SECURITY CLASSIFICATION OF FORM
(highest classification of Title, Abstract, Keywords)

DOCUMENT CONTROL DATA

(Security classification of title, body of abstract and indexing annotation must be entered when the overall document is classified)

1. ORIGINATOR (the name and address of the organization preparing the document. Organizations for whom the document was prepared, e.g. Establishment sponsoring a contractor's report, or tasking agency, are entered in section 8.)

Defence Research Establishment Pacific
FMO Victoria, BC
V0S 1B0

2. SECURITY CLASSIFICATION (overall security classification of the document including special warning terms if applicable)

UNCLASSIFIED

3. TITLE (the complete document title as indicated on the title page. Its classification should be indicated by the appropriate abbreviation (S,C,R or U) in parentheses after the title.)

A Damage Tolerance Assessment of Bonded Repairs to CF-18 Composite Components.
Part I: Adhesive Properties

4. AUTHORS (Last name, first name, middle initial. If military, show rank, e.g. Doe, Maj. John E.)

Russell, Alan J.

5. DATE OF PUBLICATION (month and year of publication of document)	6a. NO. OF PAGES (total containing information. Include Annexes, Appendices, etc.)	6b. NO. OF REFS (total cited in document)
December 1988	27	10

7. DESCRIPTIVE NOTES (the category of the document, e.g. technical report, technical note or memorandum. If appropriate, enter the type of report, e.g. interim, progress, summary, annual or final. Give the inclusive dates when a specific reporting period is covered.)

DREP Technical Memorandum

8. SPONSORING ACTIVITY (the name of the department project office or laboratory sponsoring the research and development. Include the address.)

DREP

9a. PROJECT OR GRANT NO. (if appropriate, the applicable research and development project or grant number under which the document was written. Please specify whether project or grant)	9b. CONTRACT NO. (if appropriate, the applicable number under which the document was written)

10a. ORIGINATOR'S DOCUMENT NUMBER (the official document number by which the document is identified by the originating activity. This number must be unique to this document.)	10b. OTHER DOCUMENT NOS. (Any other numbers which may be assigned this document either by the originator or by the sponsor)
DREP TM 88-25	

11. DOCUMENT AVAILABILITY (any limitations on further dissemination of the document, other than those imposed by security classification)

(X) Unlimited distribution
( ) Distribution limited to defence departments and defence contractors; further distribution only as approved
( ) Distribution limited to defence departments and Canadian defence contractors; further distribution only as approved
( ) Distribution limited to government departments and agencies; further distribution only as approved
( ) Distribution limited to defence departments; further distribution only as approved
( ) Other (please specify):

12. DOCUMENT ANNOUNCEMENT (any limitation to the bibliographic announcement of this document. This will normally correspond to the Document Availabilty (11). However, where further distribution (beyond the audience specified in 11) is possible, a wider announcement audience may be selected.)

UNCLASSIFIED

SECURITY CLASSIFICATION OF FORM

DCD03 8/04/87

13. ABSTRACT (a brief and factual summary of the document. It may also appear elsewhere in the body of the document itself. It is highly desirable that the abstract of classified documents be unclassified. Each paragraph of the abstract shall begin with an indication of the security classification of the information in the paragraph (unless the document itself is unclassified) represented as (S), (C), (R), or (U). It is not necessary to include here abstracts in both official languages unless the text is bilingual).

The damage tolerance behaviour of three epoxy adhesives used in the manufacture and repair of the composite structure on the CF-18 aircraft is assessed. The resistance to both static fracture and fatigue crack growth are evaluated. Experimental variables include the mode of fracture (tension and shear), the fatigue load ratio, the test temperature and the method of bonding. Both the static and fatigue tests were found to rank the adhesives in the same order, viz. FM-300K superior to FM-300 superior to EA-9321. The fatigue testing revealed a tendency for delamination type failures to occur at low temperature, a situation likely to lead to non-conservative joint designs. The results are discussed in terms of the failure mechanisms observed and the implication of these findings to the selection of repair adhesives for composite aircraft structure is discussed.

14. KEYWORDS, DESCRIPTORS or IDENTIFIERS (technically meaningful terms or short phrases that characterize a document and could be helpful in cataloguing the document. They should be selected so that no security classification is required. Identifiers, such as equipment model designation, trade name, military project code name, geographic location may also be included. If possible, keywords should be selected from a published thesaurus. e.g. Thesaurus of Engineering and Scientific Terms (TEST) and that thesaurus identified. If it is not possible to select indexing terms which are Unclassified, the classification of each should be indicated as with the title.)

repair
bonded joint
adhesive
epoxy
fracture
fatigue
crack growth
damage tolerance
durability
composite materials
graphite/epoxy
aircraft